Eur. J. Mineral.
2014, **26**, 103–111
Published online January 2014

Laachite, $(Ca,Mn)_2Zr_2Nb_2TiFeO_{14}$, a new zirconolite-related mineral from the Eifel volcanic region, Germany

NIKITA V. CHUKANOV[1,*], SERGEY V. KRIVOVICHEV[2], ANNA S. PAKHOMOVA[2], IGOR V. PEKOV[3], CHRISTOF SCHÄFER[4], MARINA F. VIGASINA[3] and KONSTANTIN V. VAN[5]

[1] Institute of Problems of Chemical Physics, Chernogolovka, Moscow Region 142432, Russia
*Corresponding author, e-mail: chukanov@icp.ac.ru
[2] Faculty of Crystallography, St. Petersburg State University, Universitetskaya Nab. 7/9, St Petersburg 199034, Russia
[3] Faculty of Geology, Moscow State University, Vorobievy Gory, 119991 Moscow, Russia
[4] Südwestdeutsche Salzwerke AG, Salzgrund 67, 74076 Heilbronn, Germany
[5] Institute of Experimental Mineralogy, Russian Academy of Sciences, Chernogolovka, Moscow Region 142432, Russia

Abstract: The new mineral laachite was discovered in a sanidinite specimen from the Laach Lake (Laacher See) volcano, Eifel region, Rheinland-Pfalz, Germany. Associated minerals are sanidine, allanite-(Ce), baddeleyite, haüyne, hedenbergite, intermediate members of the jacobsite-magnetite series, phlogopite, rhodonite, spessartine, tephroite, thorite, zircon, and a pyrochlore-group mineral. Laachite is deep brownish-red, has an adamantine lustre, and is translucent; the streak is brownish red. It forms long-prismatic crystals up to $0.02 \times 0.04 \times 0.5$ mm, which are present as random intergrowths and twins in cavities within sanidinite. The density calculated from the empirical formula is 5.417 g/cm^3. The mean refractive index calculated from the Gladstone-Dale relationship is 2.26. The Raman spectrum shows the absence of hydrogen-bearing groups. The chemical composition is (electron microprobe, mean of 5 analyses, wt. %): CaO 4.29, MnO 9.42, FeO 5.73, Y_2O_3 2.56, La_2O_3 2.00, Ce_2O_3 6.37, Nd_2O_3 2.22, Al_2O_3 0.99, ThO_2 7.75, TiO_2 10.98, ZrO_2 19.39, Nb_2O_5 27.82, total 99.52. The empirical formula based on 14 O atoms is: $(Ca_{0.66}Mn_{0.37}Th_{0.25}Y_{0.20}La_{0.11}Ce_{0.34}Nd_{0.11})(Zr_{1.36}Mn_{0.64})(Nb_{1.81}Ti_{1.19})(Fe_{0.69}Al_{0.17}Mn_{0.14})O_{14.00}$.

The simplified formula, taking into account the structural data, is: $(Ca,Mn)_2(Zr,Mn)_2Nb_2TiFeO_{14}$. Laachite is monoclinic, space group $C2/c$, $a = 7.3119(5)$, $b = 14.1790(10)$, $c = 10.1700(7)$ Å, $\beta = 90.072(2)°$, $V = 1054.38(1)$ Å^3, $Z = 4$. The crystal structure was solved using single-crystal X-ray diffraction data. Laachite is a monoclinic analogue of zirconolite-3*O*, $CaZrTi_2O_7$, with Nb dominant over Ti in the octahedral sites *Nb*1 and *Nb*2 and Fe dominant in a site with four-fold coordination. The strongest lines of the powder X-ray diffraction pattern [*d*, Å (*I*, %) (*hkl*)] are: 4.298 (22) (022), 2.967 (100) (20–2, 202), 2.901 (59) (042), 2.551 (32) (15–1, 151, 240, 004), 1.800 (34) (24–4, 244), 1.541 (24) (37–1, 371), 1.535 (23) (20–6, 206), 1.529 (23) (046).

Key-words: laachite, new mineral, zirconolite, sanidinite, crystal structure, alkaline volcanic rock, Laacher See, Eifel.

Introduction

The Eifel volcanic region is situated in Germany, west of the middle Rhine valley and north of the Mosel valley, and is well known for its numerous localities of young volcanic rocks of Tertiary or Quaternary age hosted by Devonian rocks. Fresh or weakly altered alkaline effusive and metasomatic rocks are exposed there in several operating quarries. Many publications are devoted to minerals and rocks of this region, including descriptions of 37 new mineral species. However, the mineralogy of late associations related to alkaline basalts and sanidinites is very complex, and thus, remains insufficiently studied.

The Laach Lake (Laacher See) volcano is situated in the centre of the East Eifel volcanic field, which is an integral part of the Rhenish Massif and may be related to the formation of the Rhine Rift system (Fuchs *et al*., 1983). Since a long time, the ejecta of the Laach Lake volcano are famous for the occurrence of rare minerals forming well-developed crystals (Nögerrath, 1808; Rath, 1861. 1871). Accessory minerals of the so-called ''nosean sanidinite'' from the Laach Lake volcano concentrate different rare elements (mainly Th, U, *REE*, Nb, and Zr). Owing to the young age of the crystallization, minerals containing radioactive elements are non-metamict and well crystalline, which enabled them to be studied in detail (Hentschel, 1990; Blass & Schäfer, 1993, 2002; Della Ventura *et al*., 2000; Chukanov *et al*., 2012a, 2012b, 2013; Kolitsch *et al*., 2012).

The present paper describes a new mineral species from the Laach Lake area, laachite named for the type locality. Both the mineral and its name have been approved by the

DOI: 10.1127/0935-1221/2013/0025-2343
0935-1221/13/0025-2343 $ 4.05

IMA Commission on New Minerals, Nomenclature and Classification (IMA no. 2012–100). Laachite is a monoclinic analogue of zirconolite-3*O*, $CaZrTi_2O_7$, with Nb dominant over Ti in two octahedral sites and Fe dominant in a site with four-fold coordination.

The type material is deposited in the collection of the Fersman Mineralogical Museum of the Russian Academy of Sciences, Moscow, Russia, with registration number 4361/1.

Occurrence, general appearance and physical properties

The holotype laachite specimen is a fragment of a vesicular sanidinite ejectum ($50 \times 30 \times 30$ cm^3), which was collected by one of the authors (Ch. S.) in one of the upper, coarse-grained layers within the pyroclastic formation of the Laach Lake volcano well known as ''Graue Laacher See Bimstuffe'' (Frechen, 1976). The outcrop is found in the active pumice quarry ''In den Dellen'' (or ''Zieglowski'' quarry), 1.5 km NE of the city of Mendig in the area of the Laach Lake, Eifel volcanic region, Rheinland-Pfalz, Germany (coordinates: 50°23'52.71'' N; 07°17'18.18''E). The fragment containing laachite has a distinctly zoned structure indicating possible metasomatic alteration of the rock.

Two associations of accessory minerals can be distinguished within the ejectum. The first one is hosted by porous sanidinite with multiple vugs between equant and tabular feldspar crystals. It includes white or colourless dodecahedra and spinel twins of haüyne, black tabular euhedral crystals (up to 1 cm) of phlogopite, black prismatic crystals of Mn-rich hedenbergite (with molar Fe:Mn:Mg $\approx$ 60:25:15), rare brownish black crystals of allanite-(Ce), thorite (typically as yellowish-green crystals and as epitactic overgrowths on zircon), and pale yellow crystals of titanite (up to 1 mm). Thorite and hedenbergite are the latest minerals in this association. The second mineral association is hosted by a denser rock, in which most gaps between the larger feldspar grains are filled by a fine-grained feldspar aggregate. It includes haüyne, intermediate members of the jacobsite–magnetite solid-solution series, laachite, baddeleyite, a pyrochlore-group mineral, spessartine, tephroite, rhodonite, titanite. In the latter association laachite and a pyrochlore-group mineral are the youngest minerals.

Laachite forms isolated, imperfect, long prismatic to acicular crystals up to $0.02 \times 0.04 \times 0.5$ mm^3 in size. They occur as random intergrowths (Fig. 1a) and as twins (Fig. 1b) in cavities in sanidinite. The twinning plane is (130); the angle between the *a* axes of the twin components is 65°. Laachite is translucent in thin fragments, otherwise deep brownish red, and it exhibits an adamantine lustre. It is brittle, with uneven fracture, and no cleavage was observed. The streak is brownish red. The density calculated from the empirical formula is 5.417 g/cm^3.

Refractive indices, 2*V,* and optical sign were not determined because only a very small amount of the mineral was available (as several tiny crystals) and because of the lack of appropriate media of suitably high refraction. The mean *n* value is 2.26, calculated from the Gladstone-Dale relationship and using the empirical formula and the calculated density. Pleochroism is medium: *a* (red-brown) $>$ *b* $\approx$ *c* (brownish red).

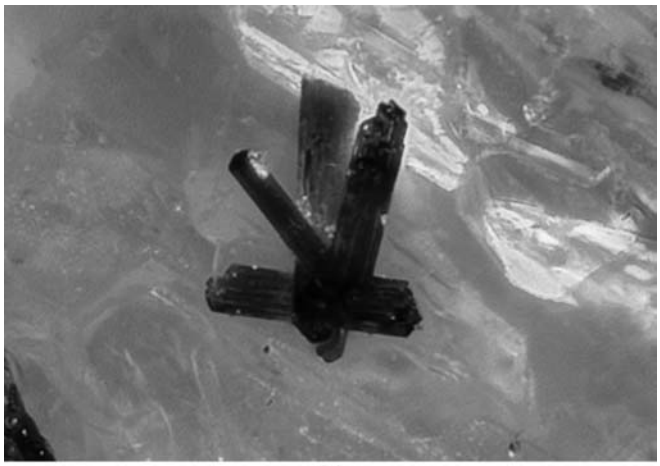
(a)

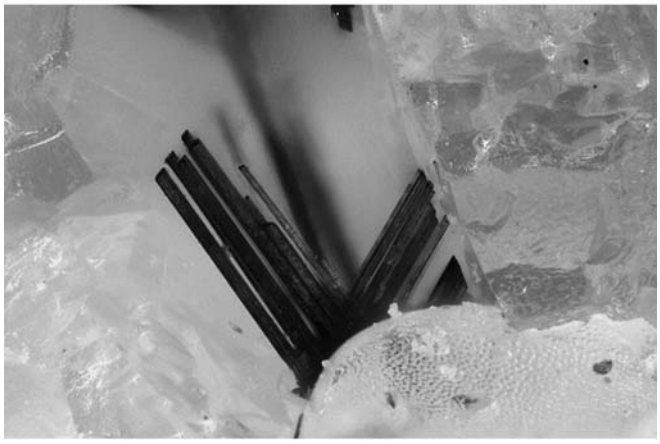
(b)

Fig. 1. (a) Cluster of laachite crystals on sanidine. View width is 0.15 mm. Photo: Bernd Gassmann. (b) Twin of laachite on sanidine. View width is 0.5 mm. Photo: Bernd Gassmann.

Raman scattering spectra of laachite were obtained at room temperature in the range from 140 to 4000 cm^{-1}, with spectral resolution about 2 cm^{-1} using a HORIBA Scientific XploRA System (Jobin Yvon) with a 1800 1/mm diffraction grating. A laser with the green exciting line at 532 nm was used with the power of the beam at the sample of approximately 6 mW. The laser beam was focused at the sample surface with a 50 $\times$ objective, and the diameter of the focal spot on the sample was $\sim$10 μm. The signal acquisition time for a single scan was 200 s, and the signal was averaged over five scans. The data processing was carried out using the LabSpec 5 program. The investigated fragment of a single crystal had the averaged linear dimensions of $\sim 60 \times 80$ μm. During the signal acquisition, the sample was lying on the plane (010); the elongation of the crystal coincides with the crystallographic axis *a*. The incident laser radiation was directed through the objective of the microscope along the axis *b*.

Raman spectra of laachite (Fig. 2a and b) show the absence of absorption bands of H_2O molecules, OH groups and CO_3^{2-} anions. Weak bands above 900 cm^{-1} presumably correspond to overtones and combination modes. Strong bands in the range 580–840 cm^{-1} are assigned to stretching vibrations of the octahedral layer, whereas those below 400 cm^{-1} correspond to lattice modes involving bending vibrations of the octahedral layer and stretching vibrations of 7- and 8-coordinated polyhedra.

Chemical data

The EDS-mode electron-microprobe analyses were carried out using VEGA TS 5130MM scanning electron microscope (SEM) equipped with an energy-dispersive X-ray (EDX) analyser (INCA Si(Li) detector), at an operating voltage of 15.7 kV and a beam current of 0.5 nA. H_2O was not analysed by any method because Raman spectroscopy data show the absence of O–H bonds. The contents of Na, Mg, Si, P, K, As, Sr, Sb, Ba, Pr, *REE* heavier than Nd, Ta, W, Pb, Bi, F, and Cl are below detection limits by EDX-analysis. With the analytical data (Table 1), the empirical formula of laachite (based on 14 O atoms) is: $Ca_{0.66}Mn_{1.15}Fe_{0.69}Al_{0.17}Y_{0.20}La_{0.11}Ce_{0.34}Nd_{0.11}Th_{0.25}Nb_{1.81}Ti_{1.19}Zr_{1.36}O_{14.00}$. Taking into account structural data (see below), this formula can be rewritten as follows: $(Ca_{0.66}Mn_{0.37}Th_{0.25}Y_{0.20}La_{0.11}Ce_{0.34}Nd_{0.11})(Zr_{1.36}Mn_{0.64})(Nb_{1.81}Ti_{1.19})(Fe_{0.69}Al_{0.17}Mn_{0.14})O_{14.00}$.

The simplified formula, taking into account the structure data (see below), is $(Ca,Mn)_2(Zr,Mn)_2Nb_2TiFeO_{14}$.

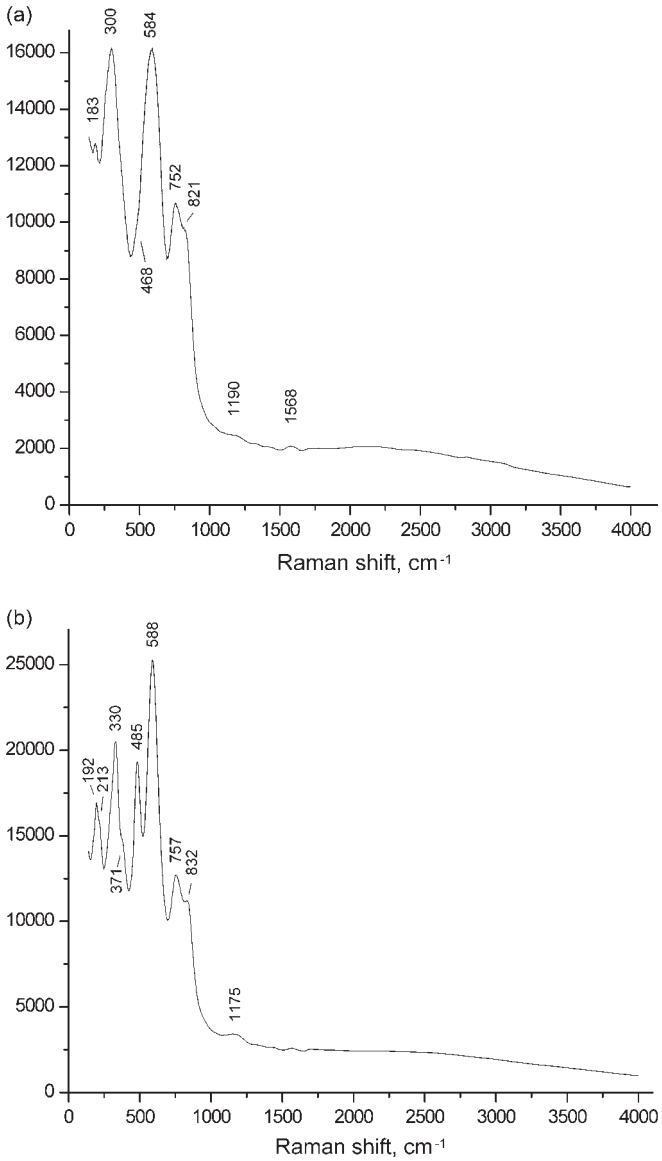

Fig. 2. (a) Raman spectrum of laachite obtained with the polarization of the laser beam parallel to the *a* axis of the crystal. (b) Raman spectrum of laachite obtained with the polarization vector of the laser beam lying in the plane (010), perpendicular to the *a* axis of the crystal.

X-ray diffraction data and crystal structure

Powder X-ray diffraction data for laachite (Table 2) were collected by means of a Stoe IPDS II Image Plate diffractometer (Gandolfi geometry) using Mo-$K\alpha$ radiation, at a distance between sample and detector of 160 mm. Diffraction peaks are well indexed in the monoclinic unit cell, space group $C2/c$. The discrepancy between $d_{obs} = 4.298$ Å and $d_{calc} = 4.132$ Å can be explained by the instrumental nonlinearity in the low-angle range when using Mo-$K\alpha$ radiation and by the high width of the reflection (002). The refined unit-cell parameters are: $a = 7.311(9)$, $b = 14.14(2)$, $c = 10.19(2)$ Å, $\beta = 90.08(2)^\circ$, $V = 1053(4)$ Å^3.

The crystal selected for single-crystal X-ray data collection was examined under an optical microscope and mounted on a glass fibre. The diffraction experiment was conducted with a Bruker APEX DUO II diffractometer equipped with a CCD (charge-coupled device) area detector. More than a hemisphere of data up to 34.99° was collected using monochromatic Mo-$K\alpha$ radiation, with a frame width of 0.5° in ω, exposure time of 30 s per frame, and a crystal-detector distance of 40.0 mm. The intensity data were integrated and corrected for Lorentz, polarization and back-ground effects using the Bruker program SAINT. The unit-cell parameters (Table 3) were refined using least-square techniques. Attempts to refine the structure in orthorhombic space groups were unsuccessful. The structure was solved by direct methods in the space group $C2/c$ and refined to $R_1 = 0.0312$. The SHELX program package was used for all structural calculations (Sheldrick, 2008). Pseudo-merohedral twinning was introduced into the model by using a matrix [-100/010/001], which improved the refinement significantly. The refined ratio between the two twin components is 0.49:0.51. The final model included all atomic positional parameters, anisotropic displacement parameters for all atoms, and a refinable weighting scheme of the structure factors. The final atomic coordinates, site occupancy factors and anisotropic displacement parameters are given in Table 4, whereas selected interatomic distances are listed in Table 5.

Table 1. Chemical composition of laachite. The mean was calculated from five SEM-EDX analyses.

Constituent	Mean, wt. %	Range, wt. %	Standard deviation, wt. %	Atomic proportions based on 14 O atoms	Standard used
CaO	4.3	4.14–4.48	0.12	0.66	Wollastonite
MnO	9.4	9.21–9.80	0.21	1.15	$MnTiO_3$
FeO	5.7	5.57–5.89	0.15	0.69	Fe
Y_2O_3	2.6	2.38–3.05	0.25	0.20	YPO_4
La_2O_3	2.0	1.58–2.44	0.30	0.11	$LaPO_4$
Ce_2O_3	6.4	6.24–6.59	0.12	0.34	$CePO_4$
Nd_2O_3	2.2	2.01–2.44	0.16	0.11	$NdPO_4$
Al_2O_3	0.99	0.92–1.07	0.04	0.17	Albite
ThO_2	7.8	6.99–8.28	0.43	0.25	ThO_2
TiO_2	11.0	10.72–11.41	0.24	1.19	$MnTiO_3$
ZrO_2	19.4	18.9–19.8	0.29	1.36	ZrO_2
Nb_2O_5	27.8	27.0–29.3	0.86	1.81	$LiNbO_3$
Total	99.5				

Table 2. X-ray powder diffraction data for laachite.

I_{obs}	d_{obs}, Å	I_{calc}	d_{calc}, Å*	*h k l*
22	4.298	7	4.132	022
16	4.055	1	4.007	11–2
		2	4.004	112
100	2.967	57	2.970	20–2
		55	2.967	202
59	2.901	100	2.908	042
8	2.661	3	2.739	22–2
		3	2.737	222
32	2.551	2	2.559	15–1
		2	2.559	151
		18	2.545	240
		10	2.543	004
8	2.335	5	2.345	223
		1	2.338	31-1
		1	2.337	311
		5	2.302	061
8	2.164	3	2.173	31-2
		3	2.171	312
		1	2.142	13–4
		1	2.140	134
9	1.955	1	1.958	313
		1	1.955	025
		1	1.948	26–1
		1	1.948	261
17	1.826	21	1.828	400
34	1.800	39	1.800	24–4
		37	1.798	244
20	1.551	12	1.548	44–2
		11	1.547	442
24	1.541	2	1.540	37–1
		2	1.540	371
23	1.535	6	1.539	20–6
		5	1.537	206
23	1.529	13	1.529	046
6	1.273	7	1.273	480
		4	1.271	008

*Calculated for unit-cell parameters obtained from single-crystal data.

Table 3. Crystallographic data and refinement parameters for laachite.

Crystal data	
Temperature	293 K
Radiation, wavelength	Mo–*K*α, 0.71073 Å
Crystal system	monoclinic
Space group	*C*2/*c*
Unit-cell dimensions *a*, *b*, *c* (Å), *β* (°)	7.3119(5), 14.1790(10), 10.1700(7) 90.072(2)
Unit-cell volume (Å^3)	1054.38(1)
Z	4
Calculated density (g/cm^3)	5.398
Absorption coefficient (mm^{-1})	15.089
Crystal size (mm^3)	0.15 × 0.03 × 0.01
Data collection	
θ range	2.00 - 34.99
h, *k*, *l* ranges	−11→ 11, −22→ 22, −16→ 16
Total reflections collected	11123
Unique reflections (R_{int})	2319 (0.026)
Unique reflections $F > 4\sigma(F)$	1974
Structure refinement	
Refinement method	Full-matrix least-squares on F^2
Weighting coefficients *a*, *b*	0.0401, 6.848
Data/restraints/parameters	2319/0/117
R_1 [$F > 4\sigma(F)$], wR_2 [$F > 4\sigma(F)$],	0.031, 0.076
R_1 all, wR_2 all	0.040, 0.083
Goodness-of-fit on F^2	1.087
Largest diff. peak and hole, e Å^{-3}	3.395, –1.449

The crystal structure of laachite contains seven crystallographically independent cation sites. The *Ca1* and *Ca2* sites are coordinated by eight oxygen atoms each, which form distorted cubes with the average <*Ca*–O> distance of 2.465 Å. The *Zr* site is coordinated by seven oxygen atoms with the average <*Zr*–O> distance of 2.190 Å. The *Nb1*, *Nb2* and *Ti* sites are octahedrally coordinated by six oxygen atoms with the average <*M*–O> distances of 1.953, 1.986 and 1.958 Å, respectively. The fourfold coordinated *Fe* position is split into two sub-sites separated by 0.762 Å. For this reason, the displacement parameters for the *Fe* site are relatively large compared to those of other atoms.

Table 4. Coordinates, site populations and displacement parameters (Å^2) of atoms in the structure of laachite.

Site	x	y	z	U_{iso}	Site population
*Nb*1	0	0.383135(7)	1/4	0.00738(2)	$Nb_{0.44}Ti_{0.40}Al_{0.16}$
*Nb*2	−1/4	3/4	0	0.01035(1)	$Nb_{0.82}Ti_{0.18}$
Ti	0	0.882243(8)	1/4	0.01061(2)	$Ti_{0.72}Nb_{0.28}$
*Ca*1	−1/2	0.631560(5)	1/4	0.00655(1)	$Ca_{0.28}Mn_{0.26}$ *Ln*$_{0.26}Th_{0.14}Y_{0.06}$
*Ca*2	0	0.632491(5)	1/4	0.00837(1)	$Ca_{0.32}Mn_{0.28}$ *Ln*$_{0.24}Th_{0.14}Y_{0.02}$
Zr	−0.24980(2)	0.483043(3)	0.013914(4)	0.00988(1)	$Zr_{0.78}Mn_{0.22}$
Fe	−0.29920(3)	0.24390(2)	−0.00901(4)	0.05016(6)	$Fe_{0.34}Mn_{0.10}Y_{0.06}$
O1	−0.25248(16)	0.62075(2)	0.08905(3)	0.00894(6)	O
O2	−0.03977(6)	0.98257(3)	0.12119(4)	0.01297(9)	O
O3	0.03600(7)	0.48118(3)	0.11947(4)	0.01699(11)	O
O4	−0.2521(2)	0.13947(2)	0.10165(3)	0.01282(7)	O
O5	−0.05679(6)	0.78155(3)	0.12714(4)	0.01263(9)	O
O6	0.05878(6)	0.28280(4)	0.12530(4)	0.01353(10)	O
O7	−0.24932(17)	0.38714(2)	0.17805(3)	0.01417(7)	O

Site	U_{11}	U_{22}	U_{33}	U_{23}	U_{13}	U_{12}
*Nb*1	0.00932(4)	0.00521(4)	0.00759(4)	0	−0.00081(3)	0
*Nb*2	0.01232(2)	0.00973(2)	0.00900(2)	0.00080(2)	−0.00182(8)	0.00234(7)
Ti	0.01009(4)	0.01288(5)	0.00887(4)	0	0.00096(3)	0
*Ca*1	0.00549(2)	0.00928(3)	0.00488(2)	0	0.00079(2)	0
*Ca*2	0.00822(2)	0.00897(3)	0.00793(2)	0	−0.00015(2)	0
Zr	0.01276(1)	0.00724(1)	0.00963(1)	−0.00205(1)	−0.00252(6)	0.00042(5)
Fe	0.07151(15)	0.03084(8)	0.04804(10)	0.02942(6)	−0.02959(16)	−0.02850(14)
O1	0.00992(11)	0.00591(11)	0.01099(11)	−0.00178(9)	0.0026(5)	−0.0029(4)
O2	0.01948(16)	0.00731(16)	0.01210(16)	0.00010(14)	−0.01300(14)	0.00180(14)
O3	0.0330(2)	0.01059(19)	0.00741(17)	0.00333(15)	−0.00825(16)	0.00126(17)
O4	0.01320(12)	0.01238(13)	0.01289(12)	−0.00182(11)	−0.0001(5)	−0.0006(4)
O5	0.02337(17)	0.00358(15)	0.01089(16)	0.00101(14)	−0.00944(14)	−0.00462(15)
O6	0.01441(16)	0.0171(2)	0.00911(16)	−0.00385(16)	0.00200(14)	0.00008(16)
O7	0.00880(11)	0.01885(15)	0.01486(13)	0.00629(12)	−0.0044(5)	0.0003(4)

Table 5. Selected interatomic distances (Å) in the structure of laachite.

*Nb*1–O3	1.9403(5) 2x	*Ca*2–O4	2.3621(12) 2x
*Nb*1–O6	1.9541(5) 2x	*Ca*2–O1	2.4713(9) 2x
*Nb*1–O7	1.9643(12) 2x	*Ca*2–O5	2.4898(5) 2x
		*Ca*2–O3	2.5368(5) 2x
*Nb*2–O6	1.9492(4) 2x		
*Nb*2–O5	1.9655(4) 2x	*Zr*–O1	2.0969(3)
*Nb*2–O1	2.0443(3) 2x	*Zr*-O4	2.0974(4)
		Zr–O2	2.1184(5)
Ti–O5	1.9419(4) 2x	*Zr*–O3	2.1323(5)
Ti–O2	1.9553(5) 2x	*Zr*–O7	2.1530(4)
Ti–O7	1.9757(12) 2x	*Zr*–O3	2.3483(5)
		Zr–O2	2.3857(5)
*Ca*1–O4	2.3830(12) 2x		
*Ca*1–O1	2.4465(9) 2x	*Fe*–O4	1.8914(6)
*Ca*1–O2	2.5025(5) 2x	*Fe*–O4	1.9400(6)
*Ca*1–O6	2.5285(5) 2x	*Fe*–O6	2.2669(5)
		Fe–O5	2.3993(5)

The crystal structure is based upon a module composed of an octahedral layer and a layer of large cations in seven- and eight-fold coordinations. The octahedral layer is built up with *Nb1*O_6, *Nb2*O_6 and *Ti*O_6 octahedra linked by corner sharing to form six- and three-membered rings (Fig. 3a). The *Fe* sites are located in the centres of six-membered rings. The second layer is composed of the *Ca*O_8 and *Zr*O_7 polyhedra. Each *Ca*O_8 polyhedron shares two opposite edges with two adjacent *Ca*O_8 polyhedra to form chains running parallel to the *a* axis. Similar chains are formed by sharing edges between the *Zr*O_7 polyhedra. Polymerization of the chains of the two types results in the formation of a dense layer (Fig. 3b). The two-layer module is formed by linkage between the octahedral layer and the layer of seven- and eightfold polyhedra (Fig. 3c). The modules are stacked along the *b* axis so that adjacent modules are rotated by 180° relative to each other (Fig. 4).

The crystal-chemical formula of laachite based upon the structural model can be written as follows ($Z = 4$, coordination numbers of cations are indicated with Roman numerals): $^{VIII}(Ca_{0.28}Mn_{0.26}$*Ln*$_{0.26}Th_{0.14}Y_{0.06})$ $^{VIII}(Ca_{0.32}Mn_{0.28}$*Ln*$_{0.24}Th_{0.14}Y_{0.02})$ $^{VII}(Zr_{1.56}Mn_{0.44})$ $^{VI}(Nb_{0.44}Ti_{0.40}Al_{0.16})$ $^{VI}(Nb_{0.82}Ti_{0.18})$ $^{VI}(Ti_{0.72}Nb_{0.28})$ $^{IV}(Fe_{0.68}Mn_{0.20}Y_{0.12})$ O_{14} or $Ca_{0.60}Mn_{1.18}Fe_{0.68}Al_{0.16}Y_{0.20}Ln_{0.50}Th_{0.28}Nb_{1.56}Ti_{1.30}Zr_{1.56}O_{14}$. This formula is in good agreement with the empirical chemical formula given above.

Laachite is a Nb-dominant monoclinic analogue of zirconolite-3*O*, the orthorhombic zirconolite polytype first described by Mazzi & Munno (1983). Zirconolite-3*O* crystallizes in the space group *Acam* with $a = 10.148(4)$ Å,

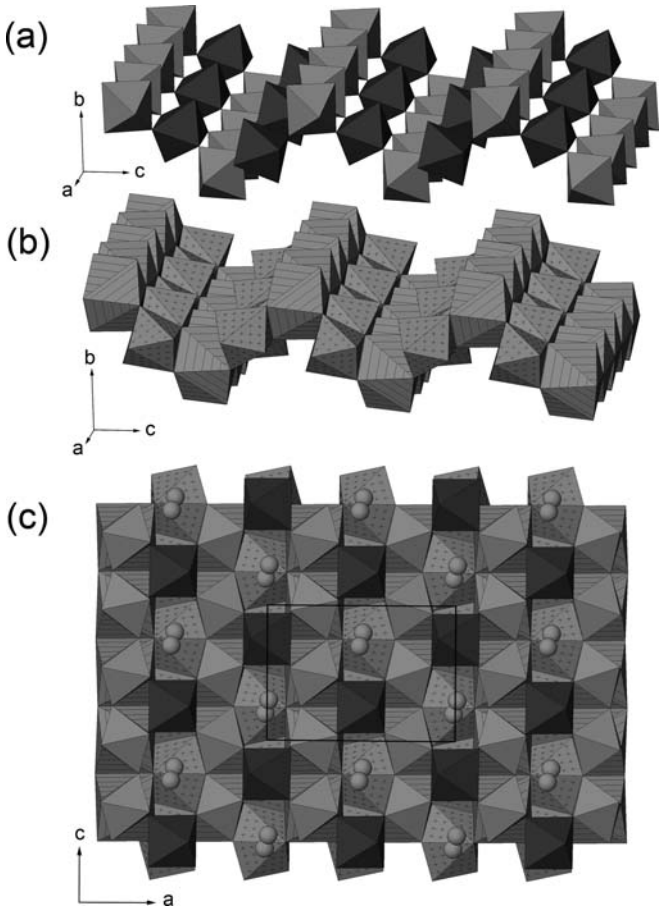

Fig. 3. Building units of the laachite crystal structure: (a) octahedral layer, (b) layer of seven- and eight-coordinated cations, (c) the module built from the octahedral and heteropolyhedral layers. Legend: *Nb*1O_6 and *Nb*2O_6 octahedra are light grey, *Ti*O_6 octahedra are dark grey, *Ca*1O_8 and *Ca*2O_8 polyhedra are light grey with lines, *Zr*O_7 polyhedra are light grey with crosses, *Fe* atoms are light grey spheres.

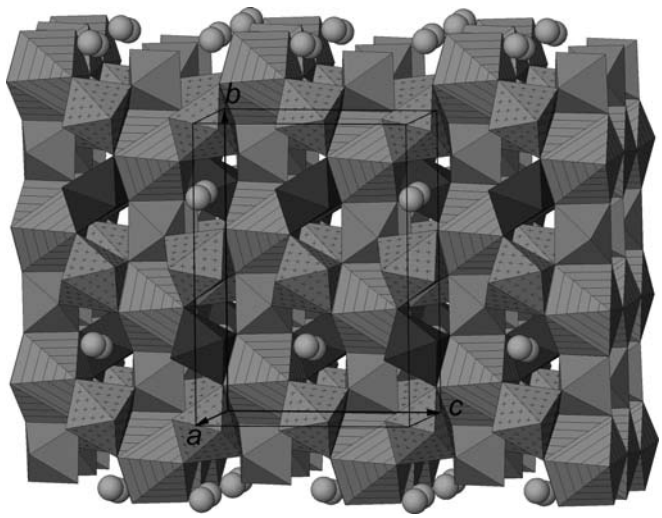

Fig. 4. The crystal structure of laachite. Legend as in Fig. 3.

$b = 14.127(5)$ Å, $c = 7.278(3)$ Å, $Z = 4$. Its crystal structure contains six cation positions: eight-fold coordinated *Me*8, seven-fold coordinated *Me*7, octahedrally coordinated *Me*6(1) and *Me*6(2), and two disordered positions, *Me*4 and *Me*5, in four- and five-fold coordination, respectively; the crystal-chemical formula of zirconolite-3*O,* based upon the site-occupancy refinement, is $^{VIII}[(Ca,Na)_{1.15}(REE,Th)_{0.85}]^{VII}(Zr_2)^{VI}[Ti_{0.52}(Nb,Ta)_{0.48}]^{VI}[Ti_{1.76}(Nb,Ta)_{0.24}]^{V}(Fe_{0.06})^{IV}(Fe_{0.92})O_{14}$. The average metal–oxygen bond distances for the *Me*8O_8 and *Me*7O_7 polyhedra are 2.460 and 2.182 Å respectively, in close agreement with the bond lengths observed in laachite. However, there are some differences in bond lengths in octahedra. The average <*Me*6(1)–O> and <*Me*6(2)–O> bond lengths are 1.978 and 1.951 Å. The *Ti*O_6 octahedron in laachite corresponds to the *Me*6(1)O_6 octahedron in zirconolite-3*O* and has a shorter average bond length ($\Delta = 0.020$ Å). The *Nb1* and *Nb2* sites in laachite correspond to the *Me*6(2) position in zirconolite-3*O*. The <*Nb1*-O> bond length is close to <*Me*6(2)–O>, with $\Delta = 0.003$ Å, whereas the <*Nb*2–O> bond is essentially longer than the <*Me*6(2)–O> bond, with $\Delta = 0.025$ Å. The observed differences in the average bond lengths are in correlation with the occupancies of corresponding sites. The *Ti* site in laachite is richer in Ti than *Me*6(1) in zirconolite-3*O*. The presence of both Nb and Al in the *Nb1* site of laachite results in an average <*Nb1*–O> bond length that is close to the one observed for the Ti-dominated *Me6*(2) position in zirconolite-3*O*. The *Nb2* position is considerably enriched in Nb, which explains the increase in the average bond length compared to the *Me*6(2) site. The crystal structure of zirconolite-3*O* is built from the layers identical to those present in laachite. Similar to laachite, the structure of zirconolite-3*O* contains disordered *Fe1* and *Fe2* sites located at the centres of six-membered rings of the octahedral layer.

Discussion and conclusions

It is a long time since Brauns (1922) and Kalb (1934, 1935, 1936, 1938) have recognized, based on the mineral associations and their replacement reactions, that the formation of sanidinites in the Laach Lake volcano was the result of two different geological processes, which led to the formation of two distinct types of highly porous feldspar rocks. One of them contains sanidine, plagioclase, as well as minor and accessory components, including blue haüyne, amphibole, pyroxene, magnetite, apatite, and titanite. The other feldspar rock type is composed mainly of potassic feldspar (usually sanidine, rarely orthoclase), with variable amounts of biotite, pyroxene, magnetite, a white or grey sodalite-group mineral (nosean or haüyne), nepheline, and cancrinite, and contains accessory rare-element minerals (zircon, zirconolite, baddeleyite, låvenite, wöhlerite, thorite, different members of the pyrochlore group, monazite, chevkinite, and allanite-group minerals). These observations led to the appearance of the terms ‘‘haüyne sanidinite’’ and ‘‘nosean sanidinite’’. The colour of the accessory sodalite-group minerals (blue or white/grey) is the most distinctive feature between the two kinds of sanidinites.

Frechen (1976) considered the ''haüyne sanidinite'' as a derivative of a haüyne-foyaite, haüyne-syenite, or haüyne-monzonite magma, and the ''nosean sanidinite'' as a derivative of a nosean-, cancrinite- or nepheline-syenite magma. Both types of porous feldspar rocks must be distinguished from the void-free sanidinite rock (sanidinite *s.s.*), which is the product of a deep alkali metasomatism of metamorphic host rocks (Frechen, 1947).

According to Schmitt *et al*. (2010), calcite-bearing noseane-syenite rocks from the Laach Lake volcano are cogenetic with the phonolitic host magma, and the crystallisation took place in an intrusive syenite-carbonatite complex at temperatures below 700 °C in the host rock surrounding the top of the magma chamber, 5000 to 20000 years prior to the eruption of the magma chamber.

Blue haüyne, the most distinctive indication for the rock of the ''haüyne sanidinite'', is absent in the laachite association. On the other hand, the rock hosting laachite contains accessory minerals that are typical for ''nosean sanidinite''.

Most samples of zirconolite enriched in Th are metamict (Williams & Gieré, 1996). In spite of a high ThO_2 content (7.75 wt. %), laachite is crystalline because of the very young age of the host rock: the last eruption of the residual phonolite magma took place at ~12.9 ka (Litt *et al*., 2001; Schmitt *et al*., 2010).

In terms of the crystal structure (Tables 4 and 5; Figs. 3 and 4), laachite is similar to zirconolite-3*O* (see Table 6). The latter was originally described under the name ''polymignite'' (Berzelius, 1824; Brøgger, 1890) and later redefined (Chukhrov & Bonshtedt-Kupletskaya, 1967; Pudovkina *et al*., 1969; Mazzi & Munno, 1983; Bayliss *et al*., 1989). ''Polymignite'' is usually metamict, and its powder X-ray diffraction pattern can be obtained only after heating.

Non-metamict zirconolite-3*O* and zirconolite-3*T* from a similar geological setting have been described by Bellatreccia *et al*. (2002). Crystals of these minerals occur in miarolitic cavities of a feldspathoid-bearing alkali-syenite ejectum collected in one of the pyroclastic flow units of the Vico volcanic complex, Italy. The age of these pyroclastic flows is estimated between 0.2 and 1.44 Ma. Transmission electron microscope studies of zirconolite crystals from the Vico complex revealed the additional presence of zirconolite-2*M* ingrowths.

A non-metamict *REE*-, Nb- and Mn-rich variety of zirconolite-3*O* was found in the Laacher See eruptive centre and described by Della Ventura *et al*. (2000). Its chemical composition varies in the following range (calculated on the basis of 14 O *apfu*): $Ca_{0.624–0.674}Y_{0.158–0.186}La_{0.138–0.172}Ce_{0.538–0.582}Pr_{0.040–0.056}Nd_{0.104–0.124}Sm_{0.008–0.012}Gd_{0.010–0.012}Dy_{0.006–0.012}Er_{0.06–0.010}Th_{0.028–0.146}U_{0.016–0.044}Mn_{0.690–0.794}Mg_{0.006–0.010}Al_{0.040–0.050}Fe_{0.602–0.678}Zr_{1.776–1.820}$

Table 6. Comparative data for laachite and zirconolite polytypes.

Mineral	Laachite	Zirconolite-2*M*	Zirconolite-3*O*	Zirconolite-3*T*
Idealized formula	$(Ca,Mn)_2(Zr,Mn)_2Nb_2TiFeO_{14}$	$CaZrTi_2O_7$	$CaZrTi_2O_7$	$CaZrTi_2O_7$
Space group	*C*2/*c*	*C*2/*c* or *Cc*	*Acam**	$P3_121$
a, Å	7.3119	12.43–12.55	10.145–10.148	7.3
b, Å	14.1790	7.22–7.23	14.147–14.18	7.3
c, Å	10.1700	11.39–11.48	7.278–7.284	16.9
β, °	90.072	100.3–100.5	90	120
Z	4	4	4	3
Strong lines of the X-ray powder diffraction pattern: *d*, Å (*I*, %)	2.967 (100)	3.176 (30)		2.98 (100)
	2.901 (59)	2.914 (100)		2.84 (20)
	2.551 (32)	2.506 (40)		2.53 (30)
	1.800 (34)	1.980 (90)		2.30 (10)
		1.792 (90)		1.82 (50)
		1.517 (10)		1.75 (30)
		(these polytypes cannot be distinguished by powder diffraction data)		1.525 (10)
				1.51 (10)
Refractive index	2.26 (mean, calc.)	2.06–2.17 (meas., metamict); 2.30–2.39 (calc.)	2.215 (meas., metamict); 2.26–2.31 (calc.)	2.39 (mean, calc.)
Density, g cm^{-3}	5.42 (calc.)	4.7 (meas.)	4.7 (meas.)	4.7 (meas.)
		4.38 (calc.)	4.9 (calc.)	5.08 (calc.)
References	This work	Borodin *et al*. 1956; Chukhrov & Bonshtedt-Kupletskaya, 1967; Pudovkina *et al*. 1969; Sinclair & Eggleton, 1982; Mazzi & Munno, 1983; Bayliss *et al*. 1989; Della Ventura *et al*. 2000.		

* Non-standard setting of the space group *Cmca*.

$Hf_{0.012–0.018}Ti_{1.680–1.776}Nb_{1.150–1.226}Ta_{0.014–0.018}Si_{0.000–0.024}O_{14}$.

A review of localities of zirconolite worldwide and a compilation of chemical compositions of about 300 samples were made by Williams & Gieré (1996). All analyses show the predominance of Ti over Nb, and for most samples the content of Nb_2O_5 is below 10 wt. %. The most Nb-rich (but Ti-dominant) zirconolite from Vuoriyarvi, North Karelia, Russia, described by Borodin *et al*. (1960) under the name ''niobozirconolite'', contains 1.596 atoms Nb and 2.162 atoms Ti per 14 O atoms. High contents of Nb are also detected in zirconolite from Kovdor, Kola Peninsula, Russia (1.304 apfu Nb at 1.714 apfu Ti), from Kaiserstuhl, Germany (1.374 apfu Nb at 1.404 apfu Ti), and from Sokli, Finland (1.216 apfu Nb at 1.546 apfu Ti) (Williams & Gieré, 1996).

On the basis of pair correlations for different components, potentially important substitutions in zirconolite have been revealed, and formulae of possible end-members have been deduced (Gieré *et al*., 1998). In particular, based on the existing compositional correlations, the following end-member formulae of zirconolite-type minerals with Nb as a species-defining component can be written: $Ca_2Zr_2Nb_2Me^{3+}{}_2O_{14}$ (Me = Fe, Al); $REE_2Zr_2Nb_2Me^{2+}{}_2O_{14}$ (Me = Fe, Mn, Mg). Chemical and structural data for laachite demonstrate the existence of a third Nb-dominant end-member, $Ca_2Zr_2Nb_2TiFeO_{14}$.

Another specific feature of the chemical composition of laachite is its high MnO content (9.42 wt. %). In most cases, the content of MnO in zirconolite is <1 wt. %. Among the ~300 zirconolite samples listed by Williams & Gieré (1996), the highest MnO content (2.0 wt. %) has been detected in zirconolite of metasomatic origin from Koberg, Bergslagen, Sweden. However, in late Nb-rich zirconolite-3*O* from the feldspar rock of the Laacher See volcano described by Della Ventura *et al*. (2000), the MnO content varies from 5.7 to 6.5 wt. %. Unlike ''haüyne sanidinites'', the ''nosean sanidinites'' of the Laacher See volcano are enriched in bulk Mn. The main minerals concentrating this element are rhodonite, spessartine, tephroite, amphiboles, pyroxenes, and members of the spinel group. The source of Mn is unknown. Taking into consideration the zoned appearance of some ''nosean sanidinitic'' ejecta (*cf.* Chukanov *et al*., 2012a), it is reasonable to assume that Mn was mobilized from surrounding metamorphic rocks.

The compositional anomalies of accessory zirconolite reflect specific features of the geochemistry of Mn-rich ''nosean sanidinites''. In this context, it is important to note that in laachite, as well as in associated accessory Mn silicates, manganese is predominantly present in the bivalent state. In the new mineral species christofschäferite-(Ce), $(Ce,La,Ca)_4Mn^{2+}(Ti,Fe^{3+})_3(Fe^{3+},Fe^{2+},Ti)(Si_2O_7)_2O_8$ (Chukanov *et al*., 2012a) and hydroxymanganopyrochlore, $(Mn^{2+},Th,Na,Ca,REE)_2(Nb,Ti)_2O_6(OH)$ (Chukanov *et al*., 2013), discovered recently in sanidinites from the Laacher See volcano, manganese is also bivalent. This fact might indicate a relatively low oxygen fugacity during the late stages of sanidinite formation.

Even though the SEM-EDX detection limits for La and Nd are rather high (0.5–0.6 wt. %), some conclusions about the proportion of rare-earth elements in laachite can be drawn. In particular, taking into account the presence of the La-dominant minerals perrierite-(La) (Chukanov *et al*., 2012b), monazite-(La) (Della Ventura *et al*., 2000), and ferriallanite-(La) (Kolitsch *et al*., 2012) in sanidinites of the Laacher See volcano, one can conclude that the low La content in laachite is connected to crystal chemical factors, but not with the geochemical environment. The ratio of rare-earth elements in laachite is in accordance with the low La affinity of the related mineral zirconolite (Yakovleva & Pekov, 2010) and its high affinity for Nd (Semenov, 1963).

Acknowledgements: The authors acknowledge partial support from the M.V. Lomonosov Moscow State University Program of Development. S.V.K. and A.S.P. were supported in this work by the Russian Federal Grant-in-Aid Program 'Cadres' (state contract 16.740.11.0490). X-ray diffraction measurements were performed in the X-ray Resource Centre of St. Petersburg State University. The authors are grateful to R. Gieré, F. Bellatreccia, and an anonymous reviewer for valuable comments and improvements.

References

Bayliss, P., Mazzi, F., Munno, R., White, T.J. (1989): Mineral nomenclature: zirconolite. *Mineral. Mag*., **53**, 565–569.

Bellatreccia, F., Della Ventura, G., Williams, C.T., Lumpkin, G.R., Smith, K.L., Colella, M. (2002): Non-metamict zirconolite polytypes from the feldspathoid-bearing alkalisyenitic ejecta of the Vico volcanic complex (Latium, Italy). *Eur. J. Mineral*., **14**, 809–820.

Berzelius J. (1824): Undersökning af några Mineralier. 2. Polymignit. *Kongl. Svenska Vetensk.-Acad. Handl.*, 338–345.

Blass, G. & Schäfer, Ch. (1993): Über eine ungewöhnliche Paragenese mit Pyrophanit und Hydrozinkit vom Laacher See. *Mineralien-Welt*, **4**(1), 14.

—, — (2002): Huttonit- und Xenotim-(Y) – Neufunde aus der Vulkaneifel. *Mineralien-Welt*, **13**(3), 32–35.

Borodin, L.S., Nazarenko, I.I., Richter, T.L. (1956): On a new mineral zirconolite – a complex oxide of AB_3O_7 type. *Dokl. Akad. Nauk SSSR*., **110**, 845–848.

Borodin, L.S., Bykova, A.V., Kapitonova, T.A., Pyatenko, Y.A. (1960): New data on zirconolite and its new niobian variety. *Dokl. Akad. Nauk SSSR*., **134**, 1188–1192.

Brauns R. (1922): Die Mineralien der niederrheinischen Vulkangebiete. N. Erwin ed., Schweizerbart, Stuttgart, 225 p.

Brøgger W.C. (1890): Die Mineralien der Syenitpegmatitgänge der südnorwegischen Augit und Nephelinsyenite. *Z. Krist. Spezieller Teil*, **16**, 1–663.

Chukanov, N.V., Aksenov, S.M., Rastsvetaeva, R.K., Belakovskiy, D.I., Göttlicher, J., Britvin, S.N., Möckel, S. (2012a): Christofschäferite, $(Ce,La,Ca)_4Mn^{2+}(Ti,Fe^{3+})_3(Fe^{3+},Fe^{2+},Ti)(Si_2O_7)_2O_8$, a new chevkinite-group mineral from the Eifel area, Germany. *New Data on Minerals*, **47**, 33–42.

Chukanov, N.V., Blass, G., Pekov, I.V., Belakovskiy, D.I., Van, K.V., Rastsvetaeva, R.K., Aksenov, S.M. (2012b): Perrierite-(La), $(La,Ce,Ca)_4Fe^{2+}(Ti,Fe)_4(Si_2O_7)_2O_8$, a new mineral species from the Eifel volcanic district, Germany. *Geol. Ore Deposits*, **54**, 647–655.

Chukanov, N.V., Blass, G., Zubkova, N.V., Pekov, I.V., Pushcharovskii, D. Yu., Prinz, H. (2013): Hydroxymanganopyrochlore: a new mineral from the Eifel Volcanic Region, Germany. *Dokl. Earth Sci*., **449**, **1**, 342–345.

Chukhrov, F.V. & Bonshtedt-Kupletskaya, E.M. (1967): Minerals. Volume II(3), Nauka, Moscow, 676 p. in Russian.

Della Ventura, G., Bellatreccia, F., Williams, C.T. (2000): Zirconolite with significant *REE*ZrNb(Mn,Fe)O_7 from a xenolith of the Laacher See eruptive center, Eifel volcanic region, Germany. *Can. Mineral*., **38**, 57–65.

Frechen, J. (1947): Vorgänge der Sanidinit-Bildung im Laacher Seegebiet. *Fortschr. Mineral*., **26**, 147–166.

— (1976): Siebengebirge am Rhein, Laacher Vulkangebiet, Maargebiet der Westeifel. Sammlung geologischer Führer. 56, 3, Auflage, Stuttgart, Schweizerbart, 209 p.

Fuchs, K., von Gehlen, K., Malzer, H., Murawski, H., Semmel, A. (1983): Plateau uplift. Springer, Berlin, 411 p.

Gieré, R., Williams, C.T., Lumpkin, G.R. (1998): Chemical characteristics of natural zirconolite. *Schweiz. Mineral. Petrogr. Mitteil*., **78**, 432–459.

Hentschel G. (1990): Die Minerale in Auswürflingen des Laacher-See-Vulkans. *Der Aufschluss, Sonderband*, **33**, 65–105.

Kalb G. (1934): Beiträge zur Kenntnis der Auswürflinge, im besonderen der Sanidinite des Laacher Seegebietes. *Mineral. Petrogr. Mitteil*., **46**, 20–55.

— (1935): Beiträge zur Kenntnis der Auswürflinge des Laacher Seegebietes II. Zwei Arten von Unbildungen Kristalliner Schiefer zu Sanidiniten. *Mineral. Petrogr. Mitteil*., **47**, 185–210.

— (1936): Beiträge zur Kenntnis der Auswürflinge des Laacher Seegebietes III. *Mineral. Petrogr. Mitteil*., **48**, 1–26.

— (1938): Beiträge zurKenntnis der Auswürflinge des Laacher Seegebietes IV. Sanidinite, deren Bildung einem nephelinsyenitischen Magma zuzuschreiben ist. *Decheniana*, **98A**(1), 1–11.

Kolitsch, U., Mills, S.J., Miyawaki, R., Blass, G. (2012): Ferriallanite-(La), a new member of the epidote supergroup from the Eifel, Germany. *Eur. J. Mineral*., **24**, 741–747.

Litt, T., Brauer, A., Goslar, T., Merk, J., Balaga, K., Mueller, H., Ralska-Jasiewiczowa, M., Stebich, M., Negendank, J.F.W. (2001): Correlation and synchronisation of Late glacial continental sequences in northern Central Europe based on annually laminated lacustrine sediments. In: Bjorck, S., Lowe, J. J., Walker, M. J. C. (eds.): Integration of Ice Core, Marine and Terrestrial Records of Termination 1 from the North Atlantic Region. *Quat. Sci. Rev*., 20, 1233–1249.

Mazzi, F. & Munno, R. (1983): Calciobetafite (new mineral of the pyrochlore group) and related minerals from Campi Flegrei, Italy; crystal structures of polymignite and zirkelite: comparison with pyrochlore and zirconolite. *Am. Mineral*., **68**, 262–276.

Nögerrath J.J. ed. (1808): Mineralogische Studien über die Gebirge am Niederrhein. Published by J.C. Hermann, Frankfurt/Main, 276 p.

Pudovkina, Z.V., Chernitzova, N.M., Pyatenko, Y.A. (1969): Crystallographic study of polymignyte. *Zapiski Vses. Mineral. Obshch*., **98**, 193–199 in Russian.

Rath G. (1861): Üeber die Krystallform des Bucklandit's (Orthit's) vom Laacher See. *Ann. Phys*., **189**, 281–292.

— (1871): Ein neues Vorkommen von Monazit (Turnerit) am Laacher-See. *Ann. Phys. Chem*., **5**, 413–420.

Schmitt, A.K., Wetzel, F., Cooper, K.M., Zou, H., Wörner, G. (2010): Magmatic longevity of Laacher See volcano (Eifel, Germany) indicated by U–Th dating of intrusive carbonatites. *J. Petrol*., **51**, 1053–1085.

Semenov E.I. (1963): Mineralogiya redkikh zemel' [Mineralogy of Rare Earth Elements]. USSR Acad. Sci, Moscow, 412 p. in Russian.

Sheldrick T.S. (2008): A short history of SHELX. *Acta Cryst*., A64, 112–122.

Sinclair, W. & Eggleton, R.A. (1982): Structure refinement of zirkelite (zirconolite) from Kaiserstuhl, Germany. *Am. Mineral*., **67**, 615–620.

Williams, C.T. & Gieré, R. (1996): Zirconolite: a review of localities worldwide, and a compilation of its chemical compositions. *Bull. Natural History Museum London (Geology)*, **52**, 1–24.

Yakovleva, O.S. & Pekov, I.V. (2010): Zirconolite family minerals in the alumina-rich fenites of the Khibiny alkaline complex (Kola Peninsula, Russia). *Abstracts of the 20th General Meeting of IMA*, Budapest, p. 438.

Received 12 July 2013
Modified version received 16 August 2013
Accepted 10 September 2013